

8-2008

Efimov states embedded in the three-body continuum

Nirav P. Mehta

Trinity University, nmehta@trinity.edu

Seth T. Rittenhouse

J.P. D’Incao

Chris H. Greene

Follow this and additional works at: http://digitalcommons.trinity.edu/physics_faculty



Part of the [Physics Commons](#)

Repository Citation

Mehta, N., Seth Rittenhouse, J. D’Incao, and Chris Greene. 2008. “Efimov States Embedded in the Three-Body Continuum.” *Physical Review A* 78 (2): 020701. doi:10.1103/PhysRevA.78.020701.

This Article is brought to you for free and open access by the Physics and Astronomy Department at Digital Commons @ Trinity. It has been accepted for inclusion in Physics and Astronomy Faculty Research by an authorized administrator of Digital Commons @ Trinity. For more information, please contact jcostanz@trinity.edu.

Efimov states embedded in the three-body continuum

N. P. Mehta,^{*} Seth T. Rittenhouse,[†] J. P. D’Incao,[‡] and Chris H. Greene[§]¹*Department of Physics and JILA, University of Colorado, Boulder, Colorado 80309-0440, USA*

(Received 13 January 2008; published 27 August 2008)

We present analytical solutions for the three-body problem with multichannel interactions and identify a class of quasibound Efimov states that can be viewed as three-body Fano-Feshbach resonances. Our method employs a multichannel generalization of the Fermi pseudopotential to model low-energy atom-atom interactions near a magnetically tunable Fano-Feshbach resonance. We discuss the conditions under which quasibound Efimov states may be supported and identify the interaction parameters that limit the lifetimes of these states. We speculate that it may be possible to observe these states using spectroscopic methods, perhaps allowing for the measurement of multiple Efimov resonances.

DOI: 10.1103/PhysRevA.78.020701

PACS number(s): 34.20.Cf, 31.15.xj

Three resonantly interacting particles can form long-range bound states, called Efimov states [1], even if the short-range interparticle interaction supports no two-body bound states. Such states are supported by an effective R^{-2} dipole potential that strongly affects few-body processes at sufficiently low energies [2–4], particularly three-body recombination, which is known to control the lifetime of trapped ultracold gases [5]. It was only recently that the first strong experimental evidence of Efimov physics was found in an ultracold thermal gas of cesium atoms [6]. The observation [6] was made possible by utilizing a magnetically tunable Fano-Feshbach resonance to precisely control the two-body scattering length a and by then observing a previously predicted [3,7,8] shape-resonant feature in the atom-loss rate due to three-body recombination. In this work, we identify a class of fully three-body Fano-Feshbach Efimov resonances embedded in the three-body continuum. Using a multichannel generalization of other models [2–4], we solve the adiabatic hyperspherical equations and analyze the resulting energy landscape.

Our model permits each atom to have multiple internal states, allowing for two-body *and* three-body scattering between different energy thresholds [9]. We note that Efimov states attached to *excited* three-body scattering thresholds are absent in single-channel models and difficult to infer from other multichannel approaches [10]. Here, our calculations show that these states are supported under the rather general stipulation that a quasibound two-body state is quasidegenerate with an excited two-body scattering threshold [11] (see Fig. 1). Given the rich structure of resonances in, for example, cesium [12], this condition could likely be satisfied. We stress that these Efimov states are of a unique character in that they can be viewed as fully three-body Fano-Feshbach resonances embedded within the three-body continuum far above the energy of open channel collisions, in contrast with the single-channel Efimov resonances predicted and recently observed that were interpreted as shape resonances [3,7]. Since the scattering length a for ground-state

atoms will not in general be resonant, the gas will be comparatively stable with respect to the a^4 overall scaling law for three-body recombination [3,5,7].

Such Efimov states attached to excited thresholds could be directly accessed via photoassociation and observed through the measurement of the resulting atom-loss rates or photoabsorption spectrum. That is, photons could be used to form these trimers directly, resulting in resonant absorption, enhancement of three-body recombination, and atom loss, thus opening a new toolkit of powerful spectroscopic techniques [13].

We let each atom have two internal states (hyperfine or Zeeman) labeled $|1\rangle$ and $|2\rangle$ with energies $E_1=0$ and $E_2=\epsilon$, respectively, where the energy splitting ϵ is a magnetically tunable parameter. Hence, the scattering of two atoms can occur between different channels labeled by symmetric products of one-atom states: $\{|\sigma\rangle\}=\{|11\rangle, (|12\rangle+|21\rangle)/\sqrt{2}, |22\rangle\}$ with respective threshold energies $\{E_{\sigma}\}=\{0, \epsilon, 2\epsilon\}$. Other two-body multichannel treatments [10] model Fano-Feshbach resonances by including a background scattering channel and a resonant molecule channel, but fail to treat the internal states of the atoms. In contrast, we label our channels explicitly by the internal states of the atoms and our Hamiltonian allows for scattering at excited energy thresholds between atoms in different internal states. Furthermore, this description is easily generalized to allow for more than two internal one-atom states.

As illustrated in Fig. 1, the zero-range s -wave two-body

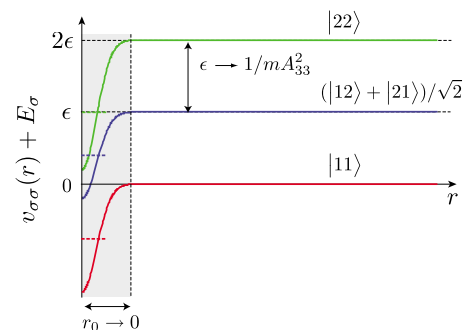


FIG. 1. (Color online) A schematic representation of our two-body model is shown. As the range r_0 is taken to zero, the potential is regularized by the derivative in Eq. (1)

^{*}mehtan@jilau1.colorado.edu[†]seth.rittenhouse@colorado.edu[‡]jpdincao@jilau1.colorado.edu[§]chris.greene@colorado.edu

potential is now written in the $\{|\sigma\rangle\}$ basis as (in atomic units which are used throughout this Rapid Communication)

$$\underline{v}(r) = \frac{4\pi\mathcal{A}}{2\mu_{2B}} \delta^3(\vec{r}) \frac{\partial}{\partial r}(r \cdot), \quad (1)$$

where $\delta^3(r)$ is the usual three-dimensional Dirac- δ function and $\mu_{2B}=m/2$ is the two-body reduced mass. This interaction is the natural extension of the regularized Fermi pseudopotential which imposes the Bethe-Peierls boundary condition on the two-body wave function, $\psi(r) \rightarrow C(1-a/r)$ as $r \rightarrow 0$. One may consider the matrix \mathcal{A} to be the multichannel generalization [14,15] of the scattering length a . When the channels in Fig. 1 are weakly coupled, \mathcal{A} is nearly diagonal with diagonal elements roughly representing background scattering lengths. A more rigorous mathematical description is obtained from multichannel quantum defect theory (MQDT) [14,16,17].

The energy-independent symmetric matrix \mathcal{A} has six independent parameters A_{ij} allowing one to explore an enormous six-dimensional parameter space. In order to simplify our analysis, we choose $A_{33}=A_{11}>0$, $A_{22}=2A_{33}$, and $A_{12}=A_{23}=A_{33}/4$. Explicitly allowing $A_{23} \neq A_{12}$ or $A_{11} \neq A_{33}$ gives qualitatively similar results in all three-body calculations described below. The particular choice $A_{22}=2A_{33}$ is made simply to illustrate the effect of a two-body quasibound state on the three-body dynamics; any $A_{22}>A_{33}$ would be sufficient for this purpose. The choice $A_{12}=A_{23}=A_{33}/4$ is arbitrary and provides strong coupling between channels modeling a broad resonance. For $A_{33}>0$, the $|22\rangle$ threshold shown in Fig. 1 supports a quasibound two-body state with energy $2\epsilon - 1/mA_{33}^2$. We show below that when this state is degenerate with the $E=\epsilon$ scattering threshold (i.e., when $\epsilon \rightarrow 1/mA_{33}^2$), an attractive R^{-2} Efimov potential appears in the three-body system near $E=\epsilon$ and $E=2\epsilon$, supporting a series of Efimov resonances.

For three atoms with positions \vec{r}_1 , \vec{r}_2 , and \vec{r}_3 , we write the mass-scaled Jacobi coordinates in the ‘‘odd-man-out’’ notation: $\vec{y}_1^{(1)}=(\vec{r}_2-\vec{r}_3)/d$ and $\vec{y}_2^{(1)}=d(\frac{\vec{r}_2+\vec{r}_3}{2}-\vec{r}_1)$ (with $d=2^{1/2}/3^{1/4}$). Other sets of Jacobi coordinates (e.g., $\{\vec{y}_1^{(2)}, \vec{y}_2^{(2)}\}$) are obtained by cyclic permutation of particles. In what follows, we omit the superscript denoting a particular choice of coordinates whenever possible. Hyperspherical coordinates are obtained by defining the hyperangle α as $\tan \alpha = |y_1|/|y_2|$, the hyperradius R as $R^2=y_1^2+y_2^2$ (which is invariant under particle permutations), and the spherical polar angles $\omega_i = \{\theta_i, \phi_i\}$ to point in the direction of \vec{y}_i . The angular coordinates $\{\alpha, \omega_1, \omega_2\}$ are collectively denoted Ω . The pairwise interactions are written in the basis of two-body internal states, with the third spectator particle (near any chosen two-particle coalescence point) in either state $|1\rangle$ or $|2\rangle$. Hence, if particle 1 is the spectator particle, we have the following six internal three-body product states: $\{|\Sigma\rangle\} = \{|111\rangle, (|112\rangle + |121\rangle)/\sqrt{2}, |211\rangle, |122\rangle, (|212\rangle + |221\rangle)/\sqrt{2}, |222\rangle\}$ with energies $\{E_\Sigma\} = \{0, \epsilon, \epsilon, 2\epsilon, 2\epsilon, 3\epsilon\}$.

In the multichannel generalization [18] of the adiabatic hyperspherical method [19], we seek solutions to the following matrix equation written in the $|\Sigma\rangle$ basis:

$$\left(\frac{\Lambda^2 + 15/4}{2\mu R^2} \mathbf{1} + E_{th} + V(R, \Omega) - U(R) \right) \vec{\Phi}(R; \Omega) = 0. \quad (2)$$

Here, Λ is the grand angular momentum operator [20], E_{th} is a diagonal matrix, $[E_{th}]_{\Sigma\Sigma'} = \delta_{\Sigma\Sigma'} E_\Sigma$, and $V(R, \Omega)$ is the sum of matrices $\underline{v}^{(k)}$ for each pairwise interaction. The three-body reduced mass is $\mu = m/\sqrt{3}$. Solutions to Eq. (2) give a spectrum of eigenvalues $U_n(R)$, which we recast in terms of a new variable $\nu_{\Sigma n}$: $\nu_{\Sigma n}(\nu_{\Sigma n} + 4) = 2\mu R^2 [U_n(R) - E_\Sigma] - 15/4$. The potentials $U_n(R)$ appear in radial equations of the form (ignoring nonadiabatic effects) $-F_n''(R)/2\mu R^2 + U_n(R)F_n(R) = EF_n(R)$.

Here, we solve Eq. (2) using a hyperangular Green’s function. The corresponding Lippmann-Schwinger (LS) equation for the Σ component of $\vec{\Phi}$ reads

$$\begin{aligned} \Phi_\Sigma(R; \Omega) = & -2\mu R^2 \sum_{\Sigma', k} \int d\Omega' G_{\Sigma\Sigma'}(\Omega, \Omega') \\ & \times v_{\Sigma\Sigma'}^{(k)}(R, \Omega') \Phi_{\Sigma'}(R; \Omega'), \end{aligned} \quad (3)$$

where components of the free-space (diagonal) hyperangular Green’s function $G(\Omega, \Omega')$ satisfy $[\Lambda^2 - \nu_\Sigma(\nu_\Sigma + 4)]G_{\Sigma\Sigma'}(\Omega, \Omega') = \delta(\Omega, \Omega')$. Postponing the full derivation to a later publication [21], we give this solution (for the first time) [22]:

$$\begin{aligned} G_{\Sigma\Sigma'}(\Omega, \Omega') = & \sum_{l_1, m_1, l_2, m_2} [g_{l_1 l_2}^{\nu_\Sigma}(\alpha, \alpha') Y_{l_1 m_1}(\omega_1) \\ & \times Y_{l_1 m_1}^*(\omega'_1) Y_{l_2 m_2}(\omega_2) Y_{l_2 m_2}^*(\omega'_2)], \end{aligned} \quad (4)$$

where $g_{l_1 l_2}^{\nu_\Sigma}(\alpha, \alpha') = N_{\nu_\Sigma l_1 l_2} f_{\nu_\Sigma l_1 l_2}^{(-)}(\alpha <) f_{\nu_\Sigma l_1 l_2}^{(+)}(\alpha >)$ and

$$\begin{aligned} f_{\nu_\Sigma l_1 l_2}^{(\pm)}(\alpha) = & (\sin \alpha)^{l_1} (\cos \alpha)^{l_2} \\ & \times {}_2F_1 \left(\frac{l_1 + l_2 - \nu_\Sigma}{2}, \frac{\nu_\Sigma + l_1 + l_2 + 4}{2}, \right. \\ & \left. l_\pm + \frac{3}{2}, \frac{1 \mp \cos(2\alpha)}{2} \right), \end{aligned} \quad (5)$$

with $l_+ = l_1$, $l_- = l_2$; l_1 (l_2) is the orbital angular momentum quantum number associated with \vec{y}_1 (\vec{y}_2). The normalization constant is $N_{\nu_\Sigma l_1 l_2} = [\Gamma(\frac{l_1+l_2-\nu_\Sigma}{2}) \Gamma(\frac{l_1+l_2+\nu_\Sigma+4}{2})] / [2\Gamma(l_1+\frac{3}{2}) \Gamma(l_2+\frac{3}{2})]$.

The LS equation (3) is then solved by evaluating the integral over $v_{\Sigma\Sigma'}^{(k)}$ in the coordinate system where $|\vec{y}_1^{(k)}| \propto |\vec{r}_i - \vec{r}_j| \propto R \sin \alpha^{(k)}$. The zero-range s -wave interaction immediately selects $l_1=0$ for the two interacting particles and $l_2=L$. For this Rapid Communication, we confine our study to states with total orbital angular momentum $L=0$. For equal-mass particles, in the limit $\alpha^{(k)} \rightarrow 0$ we have $\alpha^{(i)} = \alpha^{(j)} = \pi/3$; the LS equation reduces to a matrix equation of the form [18]

$$\left(\frac{3^{1/4}}{2^{1/2}R} (\underline{M}^{(1)} + \underline{M}^{(2)} \underline{P}_- + \underline{M}^{(3)} \underline{P}_+) - \mathbf{1} \right) \vec{C}^{(1)} = 0, \quad (6)$$

where, for bosons,

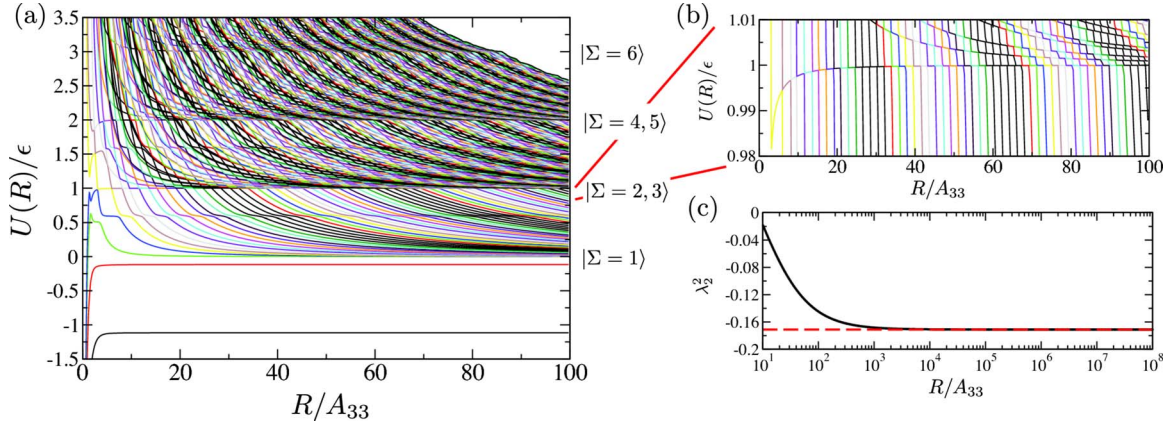


FIG. 2. (Color online) In (a), we show approximately the lowest 300 potential curves up to 3.5ϵ , while (b) shows an enlarged view of the region near the $E=\epsilon$ threshold and the attractive R^{-2} diatomic Efimov potential. Note also the series of avoided crossings in (a) near $E=0.6\epsilon$ indicating the presence of a two-body quasibound state. In (c) we show the eigenvalue near $E=\epsilon$ converging to the universal value for two identical bosons and one distinguishable particle $\lambda^2 \rightarrow -0.171145 = -s_0^2$ indicated by the dashed red line.

$$M_{\Sigma\Sigma'}^{(i)} = \begin{cases} A_{\Sigma\Sigma}^{(i)} \lambda_{\Sigma} \cot(\lambda_{\Sigma} \pi/2), & i = 1, \\ A_{\Sigma\Sigma'}^{(i)} \frac{-4 \sin(\lambda_{\Sigma} \pi/6)}{\sqrt{3} \sin(\lambda_{\Sigma} \pi/2)}, & i = 2, 3. \end{cases} \quad (7)$$

The vector associated with the n th eigenstate, $\vec{C}_n^{(1)}$ in Eq. (6), is defined by the boundary and normalization conditions

$$C_{\Sigma n}^{(k)} = \lim_{r_k \rightarrow 0} \frac{\partial(r_k \Phi_{\Sigma n})}{\partial r_k} \quad \text{and} \quad \sum_{\Sigma} \langle \Phi_{\Sigma n} | \Phi_{\Sigma n} \rangle = 1. \quad (8)$$

We have rewritten the eigenvalue as $\nu_{\Sigma} = \lambda_{\Sigma} - 2$ purely for convenience, and P_+ and P_- perform cyclic and anticyclic particle permutations, respectively, upon the basis $\{|\Sigma\rangle\}$. Zeros of the determinant of the matrix in Eq. (6) yield the eigenvalues $\lambda_{\Sigma n}^2 = 2\mu R^2 [U_n(R) - E_{\Sigma}] + 1/4$.

As mentioned before, by allowing ϵ to vary with the magnetic field, it is possible to make a quasibound two-body state degenerate with the $|\sigma=2\rangle$ threshold. This occurs when $\epsilon \rightarrow 1/(mA_{33}^2)$ as illustrated in Fig. 1. Under these conditions, provided that $|A_{13}| \ll A_{33}$, an Efimov potential appears at both the $E=\epsilon$ and $E=2\epsilon$ three-body thresholds. In Fig. 2(a) we show the lowest 300 adiabatic potential curves up to $E=3.5\epsilon$. Note the collection of three-body curves converging to the various three-body scattering thresholds $\{E_{\Sigma}\}$, corresponding asymptotically to three free atoms in internal states given by $\{|\Sigma\rangle\}$. In Fig. 2(b), which shows in detail the three-body potentials near $E=\epsilon$, the Efimov potential appears as an attractive *diatomic* potential connected through a series of sharp avoided crossings. The eigenvalues $\lambda_2^2 = \lambda_1^2 - 2\mu R^2 \epsilon$ corresponding to this diatomic potential are shown in Fig. 2(c) to converge to the universal value $\lambda_2^2 \rightarrow -0.171145 = -s_0^2$. Note that this universal value is appropriate for two identical bosons interacting resonantly with a third distinguishable particle of equal mass [24,25] and is consistent with the fact that the $E=\epsilon$ threshold corresponds to atoms in internal states $(|112\rangle - |121\rangle)/\sqrt{2}$ and $|211\rangle$.

The lifetime of Efimov states near $E=\epsilon$ is limited by the lifetime of the resonant two-body quasibound state (see Fig. 1). We find for $A_{13} \ll A_{33}$ that the quasibound two-body state

lifetime scales as $(A_{33}/A_{13})^4$. This two-body lifetime in turn controls the radial widths of avoided crossings at large R . This is understood qualitatively by noting that when A_{13} is sizable, direct inelastic transitions between $|\sigma=3\rangle$ and $|\sigma=1\rangle$ states dominate over two-step transitions via the intermediate $|\sigma=2\rangle$ state, where the presence of the quasibound two-body state at energy $E=\epsilon$ strongly affects the three-body dynamics. In the limit $A_{13} \rightarrow 0$, we find that inelastic transitions will occur only for $R \lesssim A_{33}$ due to broader avoided crossings whose widths are controlled by the couplings A_{12} and A_{23} . If all transitions occur at short range, the width of each successive Efimov state scales with the same geometric factor as the energy: $\Gamma_n/\Gamma_{n-1} = E_n/E_{n-1} = e^{-2\pi/s_0}$.

Experimentally, the resolution of spectroscopic techniques is limited by the lifetime of the gas. In the present scheme, atoms spend time near $E=0$, where the interaction is not resonant and the gas is expected to be stable with respect to the approximate a^4 scaling law for three-body recombination. Photons with energy $\hbar\omega = E_n < \epsilon$ are then introduced to associate Efimov trimers directly. Note that since $\hbar\omega < \epsilon$, two-body collisions at the $E=\epsilon$ threshold are not energetically allowed. It may be possible, therefore, to probe Efimov resonances attached to excited three-body thresholds for times long enough to resolve a second resonant feature in either photoabsorption or atom loss. Further, the geometric scaling factor $e^{-2\pi/s_0}$ could be made more favorable by either using heteronuclear mixtures of atoms, capitalizing on mass ratios different from unity [1,25,26], or by considering atoms with more than two internal states and placing a quasibound two-body state at a scattering threshold of the form [22], recovering the bosonic scaling factor $e^{-2\pi/s_0} \approx 22.7$.

In order for the Efimov states to persist, it is sufficient to show that the positive-definite adiabatic correction $-Q(R) = -\langle \Phi(R) | \frac{\partial^2}{\partial R^2} | \Phi(R) \rangle$ corresponding to the Efimov potential falls off faster than R^{-2} . Following a multichannel generalization of the method used in [23], we find that this correction for the Efimov potential falls off as R^{-3} , consistent with the single-channel result and allowing these states to persist.

In Fig. 2(a), the series of avoided crossings near 0.6ϵ is a

direct result of the quasibound two-body state attached to the $|\sigma=2\rangle$ threshold in Fig. 1. The radial width of these avoided crossings is controlled by the width of the two-body resonance. For a broad resonance, three-body collisions near this energy couple strongly to the two-body Fano-Feshbach resonance through this series of avoided crossings. As the two-body resonance becomes narrower, the avoided crossings become sharper, converging to a true atom-dimer scattering threshold in the limit of an infinitely narrow resonance. Note that the degeneracy of a quasibound two-body state with the $E=0$ scattering threshold results in the usual Fano-Feshbach resonance and leads to the series of Efimov states that were interpreted as shape resonances in Ref. [6].

To summarize, we have identified a class of Efimov states embedded in the three-body continuum. The hyperradial potentials supporting these states have universal properties consistent with the symmetry constraints implied by the internal degrees of freedom of the three-atom system and can further

be understood in terms of relevant two-body length scales. Further, we have identified the parameter A_{13} responsible for the long-range coupling which limits the lifetime of these Efimov states and have found that the repulsive diagonal nonadiabatic correction falls off as R^{-3} , consistent with the single-channel result. We stress that since the potential supporting these states appears when a quasibound two-body state is degenerate with an *excited* two-body threshold, the open-channel scattering length in general will not be resonant, and the gas is expected to be stable with respect to the general a^4 scaling of recombination. We postulate that it may be possible to observe these states by spectroscopic techniques, perhaps with sufficient accuracy to measure two Efimov resonances.

We thank D. Blume and J. H. Macek for useful discussions during the early stages of this work. This work is supported by the National Science Foundation.

-
- [1] V. Efimov, *Sov. J. Nucl. Phys.* **10**, 62 (1970).
 [2] E. Nielsen *et al.*, *Phys. Rep.* **347**, 373 (2001).
 [3] B. D. Esry, C. H. Greene, and J. P. Burke, *Phys. Rev. Lett.* **83**, 1751 (1999).
 [4] J. P. D’Incao and B. D. Esry, *Phys. Rev. Lett.* **94**, 213201 (2005).
 [5] E. Braaten and H.-W. Hammer, *Phys. Rep.* **428**, 259 (2006).
 [6] T. Kraemer *et al.*, *Nature (London)* **440**, 315 (2006).
 [7] E. Nielsen and J. H. Macek, *Phys. Rev. Lett.* **83**, 1566 (1999).
 [8] E. Braaten and H.-W. Hammer, *Phys. Rev. Lett.* **87**, 160407 (2001).
 [9] A “threshold” is the energy at which a particular scattering process becomes energetically allowed.
 [10] M. D. Lee, T. Kohler, and P. S. Julienne, *Phys. Rev. A* **76**, 012720 (2007).
 [11] This stipulation has a caveat that in the matrix \underline{A} of Eq. (1), $A_{13} \ll A_{33}$.
 [12] C. Chin *et al.*, *Phys. Rev. A* **70**, 032701 (2004).
 [13] J. Léonard *et al.*, *Phys. Rev. Lett.* **91**, 073203 (2003); C. A. Regal *et al.*, *Nature (London)* **424**, 47 (2003); S. Gupta *et al.*, *Science* **300**, 1723 (2003); M. Bartenstein *et al.*, *Phys. Rev. Lett.* **94**, 103201 (2005).
 [14] M. H. Ross and G. L. Shaw, *Ann. Phys.* **13**, 147 (1961).
 [15] R. C. Forrey, N. Balakrishnan, V. Kharchenko, and A. Dalgarno, *Phys. Rev. A* **58**, R2645 (1998).
 [16] M. Aymar, Chris H. Greene, and Eliane Luc-Koenig, *Rev. Mod. Phys.* **68**, 1015 (1996).
 [17] J. P. Burke, C. H. Greene, and J. L. Bohn, *Phys. Rev. Lett.* **81**, 3355 (1998).
 [18] O. I. Kartavtsev and J. H. Macek, *Few-Body Syst.* **31**, 249 (2002); J. H. Macek, *ibid.* **31**, 241 (2002).
 [19] J. H. Macek, *J. Phys. B* **1**, 831 (1968).
 [20] J. Avery, *Hyperspherical Harmonics: Applications in Quantum Theory* (Kluwer Academic, Norwell MA, 1989).
 [21] N. P. Mehta, Seth T. Rittenhouse, and Chris H. Greene (unpublished).
 [22] The Green’s function is known in terms of an eigenfunction expansion: M. Fabre de la Ripelle, *Few-Body Syst.* **14**, 1 (1993). A closed-form solution has been found in R. Szmajkowski, *J. Phys. A* **40**, 995 (2007).
 [23] O. I. Kartavtsev and A. V. Malykh, *Phys. Rev. A* **74**, 042506 (2006); *J. Phys. B* **40**, 1429 (2007).
 [24] A. Bulgac and V. Efimov, *Sov. J. Nucl. Phys.* **22**, 153 (1976).
 [25] V. Efimov, *Nucl. Phys. A* **210**, 157 (1973).
 [26] J. P. D’Incao and B. D. Esry, *Phys. Rev. A* **73**, 030703(R) (2006).